Proceedings of IMECE2008
ASME International Mechanical Engineering Congress and Exposition
November 2-6, 2008, Boston, Massachusetts, USA

IMECE2008-69143

A HARDWARE-IN-THE-LOOP SIMULATION TESTBED FOR EMULATING HYDRAULIC LOADS REPRESENTING THE COMPLETE DIG CYCLE OF A CONSTRUCTION MACHINE

Aaron R. Enes
Woodruff School of Mechanical Engineering
Georgia Institute of Technology
Atlanta, GA 30318
aaron.enes@gatech.edu

Wayne J. Book
Woodruff School of Mechanical Engineering
Georgia Institute of Technology
Atlanta, GA 30318
wayne.book@me.gatech.edu

ABSTRACT

A hardware-in-the-loop (HIL) simulation testbed is designed to be capable of emulating the entire domain of hydraulic workport loads incident on a test valve during normal work cycle operations of a certain hydraulic construction machine, such as a backhoe or excavator. The HIL testbed is a useful tool during rapid prototyping of control algorithms for the test valve, and for performing controlled experiments with the valve in the context of developing valve control algorithms to improve the overall energy efficiency of hydraulic systems. This paper discusses four key topics: the architecture of the real-time simulation and testbed control process, the modeling and validation of the emulated machine dynamics, the controller development for the HIL testbed, and some initial performance testing of the HIL testbed.

INTRODUCTION

Hydraulic hardware has undergone a great evolution in recent years, evolving from purely hydro-mechanical devices to electro-hydraulic systems controlled by microprocessors. The use of electronic controllers opens the door to improving dynamic performance and enhancing traditional hydraulic off-highway construction machines with new features such as increased energy efficiency, improved operator controllability, and overall increases in productivity. With these added capabilities often comes added system complexity, particularly in the area of system controls. To help aide in the rapid development of these new complex control systems, we developed a hardware-in-the-loop (HIL) testbed for emulating the hydraulic loads incident on a certain control valve during operation. This testbed is a useful tool for design engineers seeking to develop more efficient and effective control algorithms for hydraulic machines. The testbed is unique because of its simple construction and inherent ability to emulate static, resistive, and overrunning loads of two-port actuation systems with differential areas, such as hydraulic cylinders, where the flow rates into and out of the actuator are unequal.

In this case, the test article, or plant, is an arrangement of electro-hydraulic poppet valves (EHPVs) of the sort developed recently at HUSCO International by Pfaff and Tabor [1] for independent metering control (IMC) of actuators in, for example, mobile hydraulic construction equipment. Also reference Tabor [2] for an application discussion of IMC technology.

This paper is organized as follows: Background, HIL System Architecture, High-level control, Low-level control development, Results of initial load emulation experiments.

HIL SIMULATION BACKGROUND

Define a system as a plant combined with an environment with which the plant interacts. Consider a mobile hydraulic construction vehicle, such as an excavator, and suppose the plant in this example is a hydraulic control valve (comprising the hydro-mechanical valve and the valve electronic controller). Then, define the environment as the remaining hydro-mechanical parts of the construction machine (e.g. hydraulic cylinder, prime mover, articulated components, etc.), plus the earthen volume in which it digs.

Suppose we wish to model and simulate the plant-environment system. In traditional computational simulations, all of the components of the modeled system—that is, both the plant and the environment—exist *in silico*, i.e. running on a computer; whereas a full-scale prototype experiment would naturally contain only real hardware. In contrast, a HIL simulation has some subset of the system as real components being connected to a computer simulation in a real-time simulation loop. The HIL testbed enables this plant/simulation interface. Hence, a computer *model* of the environment and the *real*, physical plant together model the system; actual hardware replaces some of the components of the traditional, purely numerical simulation. The environment simulation occurs in the same loop as the plant's physical response; thus, the input and output signals of the simulated

environment are controlled to execute time-dependent values matching the real environment. The simulation part computes the system dynamics of the real environment from a mathematical model, and then—accounting for the dynamics of the hardware comprising the plant/simulation interface—the HIL testbed "displays" these input and output signals on the plant. The interface must convert signals from the computer simulation domain to the analog power domain of the plant (in this case, hydraulic pressure and flow).

Certainly, increased computing power now enables rapid simulation of very complex system models: Models can be created and simulated with high order to represent most predictable behaviors. However, the drawback of relying on pure software simulation is that some unexpected behaviors, i.e. high-order resonances or failure modes, may not be captured by models used in first-iteration system designs. Simulations are doomed to succeed, and a false sense of confidence born from a successful simulation can be destroyed by a single experiment using real plant hardware. A HIL simulation enables testing over the full range of operating conditions, including failure modes too dangerous to test otherwise, while removing the variability of the operating environment.

Other Hydraulic HIL Testbeds

There have been several hydraulic HIL testbeds constructed and used by various researchers for rapid prototyping tasks, as briefed in Table 1. The testbeds are broadly categorized as either *active* by the ability to add or remove power from the test article (and thereby possibly emulate both resistive and overrunning loads), or *passive* if it is only capable of removing power from the test article (hence only able to emulate resistive loads). Further, the testbed can be described by the number of energy ports it is able to operate on (e.g. an engine dynomoter may emulate loads on only one port, the drive shaft; while the hydraulic loads on a control valve may simultaneously act on two ports connected to the head- or rod-side of a cylinder).

HIL SYSTEM ARCHITECTURE

The plant in this work is an arrangement of four electro-hydraulic poppet valves (EHPVs) of the type used for independent metering control of a hydraulic cylinder. Figure 1 is a schematic of the test valve with the plant/environment interfaces depicted: workports (A) and (B), pressure supply port (P_s), and interface for the EHPV control signals (C). Assume the port draining to tank is held at constant pressure.

TABLE 1. OTHER HYDRAULIC HIL TESTBEDS

Zhang, Carter and Alleyne [3]	Passive testbed. Uses an electro-hydraulic valve to meter out flow, thereby controlling the power removed from the system.
Lahti, Andrasko and Moskwa [4].	Active testbed. Capable of emulating a single energy port, in this case it emulates the torque-speed loads on a test engine shaft.
C. Ramden [5].	Active testbed. Can add or remove energy on two energy ports per testbed. The ability to emulate static loads is uncertain.
Driscoll, Huggins and Book [6]	Active testbed. Capable of 2-port load emulation. Emulates static and dynamic loads, and is capable of adding or removing energy from test article.

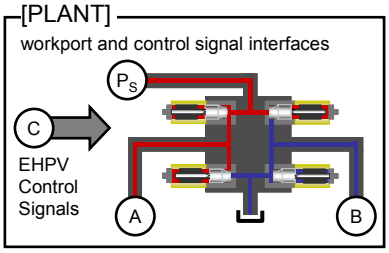

FIGURE 1. ACTUAL PLANT CONSISTING OF FOUR EHPVS AND PLANT/ENVIRONMENT INTERFACES:WORKPORTS (A) AND (B), PRESSURE SUPPLY PORT (P_S), AND CONTROLLER INTERFACE (C)

A possible operating environment of the plant is in controlling the arm function of an excavator, as depicted in Figure 2, where interfaces (A), (B), (C), and (P_S) of the environment connect to the corresponding ports of the actual plant described in Figure 1. The block "Actual Controller" controls the EHPVs and the system pressure as a function of the operator velocity command (V_{cmd}) and the sensed workport pressure, i.e. the block may implement a manufacturer's proprietary control logic as described by Pfaff and Tabor [1]. Assume the hydraulic pressure-flow dynamics at workports (A) and (B) are a function of the fluid and cylinder properties, the rigid body dynamics of the machine, and the digging loads. These dynamics define the relationship between pressure and flow and will be referred to as the "workport signature" of the machine. The workport signature is used to describe how the flow response through the workports varies as a function of the workport pressure.

During typical dig cycles, the plant is subject to three general classes of loads: overrunning, resistive, and static. Figure 3 shows portions of a sample excavation dig cycle that belong to each classification.

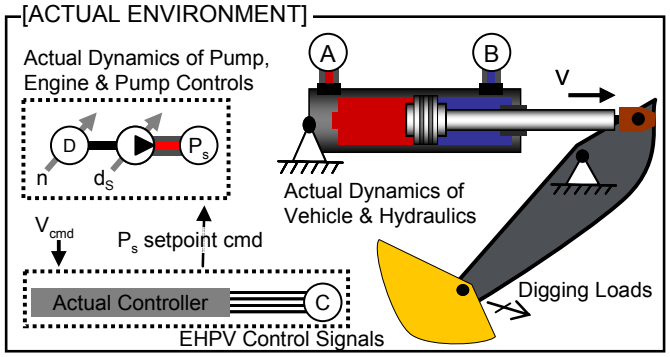

FIGURE 2. NORMAL OPERATING ENVIRONMENT OF THE PLANT

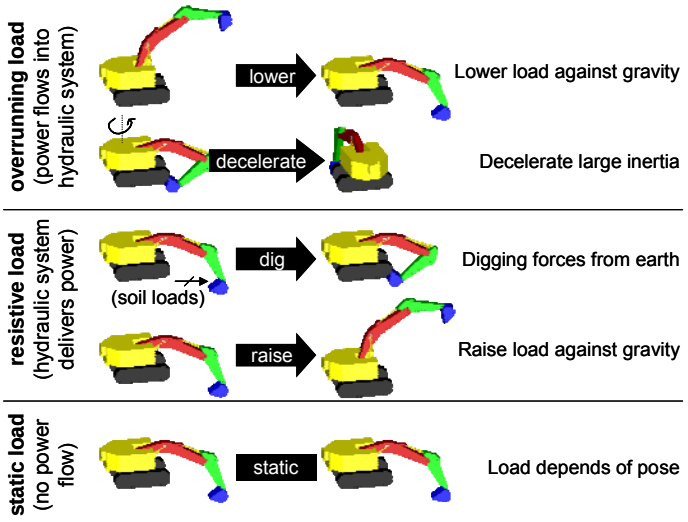

FIGURE 3. THREE TYPICAL VALVE LOADING CONDITIONS DURING A DIG CYCLE

The architecture of the HIL system discussed here was chosen so that a workport signature comprising all three classes of loads could be emulated. The emulated plant environment is produced by detaching the plant from the actual environment and instead connecting the plant to the testbed interfaces depicted in Figure 4.

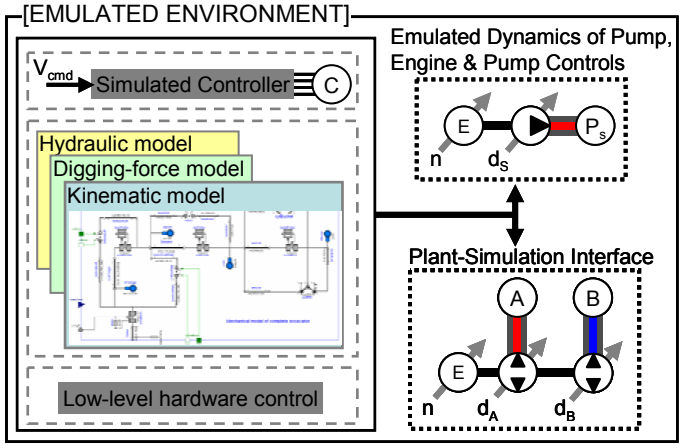

FIGURE 4. HIL SYSTEM USED TO IMPLEMENT THE EMULATED PLANT ENVIRONMENT

The emulated plant environment consists of one software system and two hardware systems. One hardware system emulates the pump/prime mover dynamics (P_S) and the other emulates the workport loads at ports (A), (B). The software system itself has three subsystems: execution of the Hydraulic Valve Controls Model, simulation of real plant environment (the Vehicle Model), and handling of low-level HIL testbed controls. In this case, low-level hardware controllers command the set of variable displacement pump/motors to produce a given workport signature having pressure/flow dynamics mimicking the real environment. These devices may act in either a pumping or motoring mode to add or remove energy from the plant.

During operation, the sensed workport pressures (P_a, P_b in Figure 5) are applied to the environment simulation. The simulated response (i.e. flow into the simulated cylinder) is used as the reference command to the low level hardware control to control the workport flows (Q_a, Q_b) through the plant.

Figure 5 is a schematic of the HIL testbed. The testbed components are shown in a cartoon and photograph in Figure 6 and Figure 7 respectively.

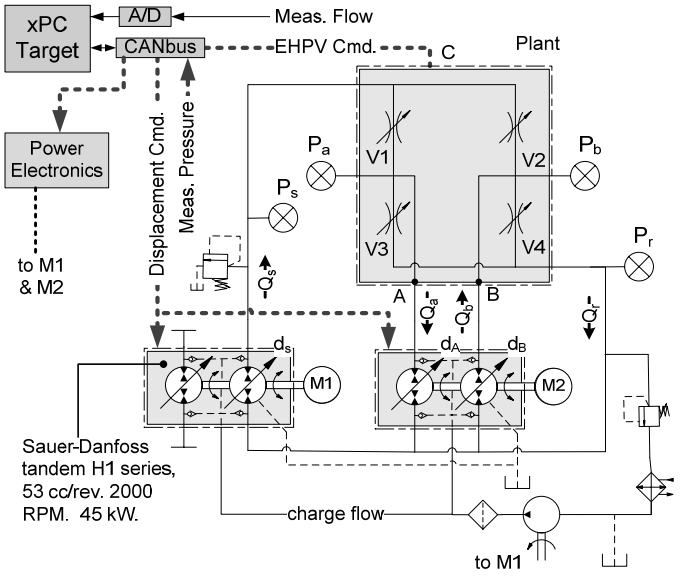

FIGURE 5. SCHEMATIC OF HIL TESTBED WITH A FOUR EHPV PLANT INSTALLED

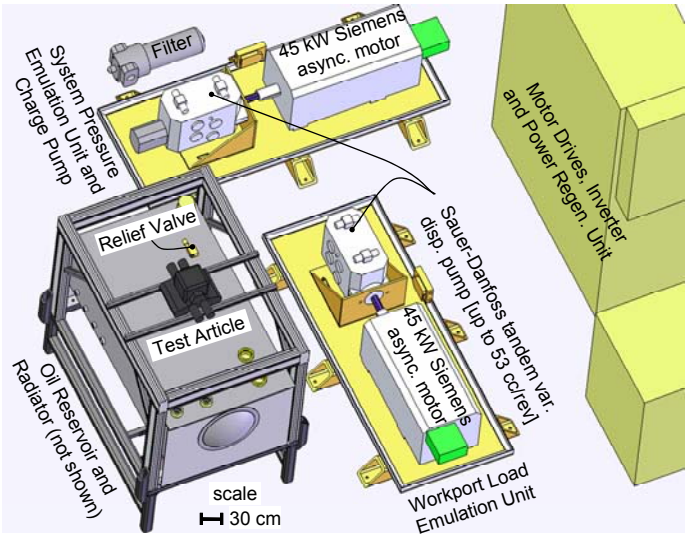

FIGURE 6. CARTOON OF THE HIL EMULATION FACILITY (PLUMBING NOT SHOWN)

Data and Signal Flow in the HIL Testbed

Figure 8 shows a high-level view of the data flow within the testbed controller. Everything within the "xPC Target – Real-time

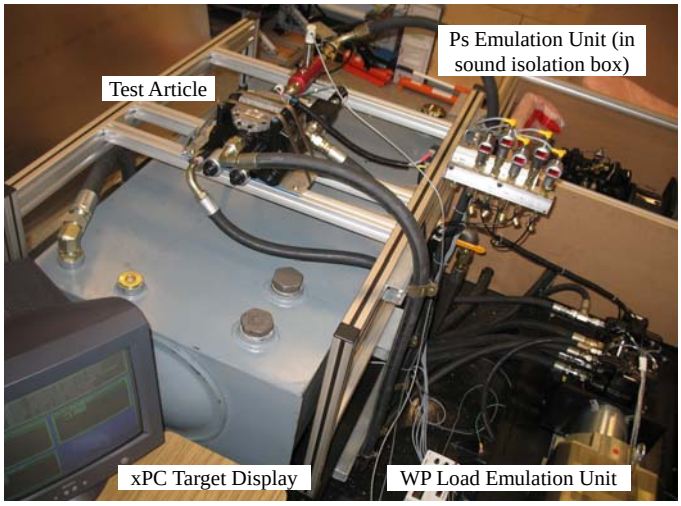

FIGURE 7. PHOTOGRAPH OF THE HIL EMULATION FACILITY

simulation control loop" operates in near real-time on a MATLAB xPC Target machine (1.2 GHz processor, 512 MB RAM). Signals for control and monitoring are transmitted via CANbus and an A/D interface. The models for the environment and the plant controller designs are created off-line in, for example, Dymola/Modelica (Dynasim [7]), and then compiled in C for execution on the xPC Target OS during the simulation. (The model development is discussed in the next section.)

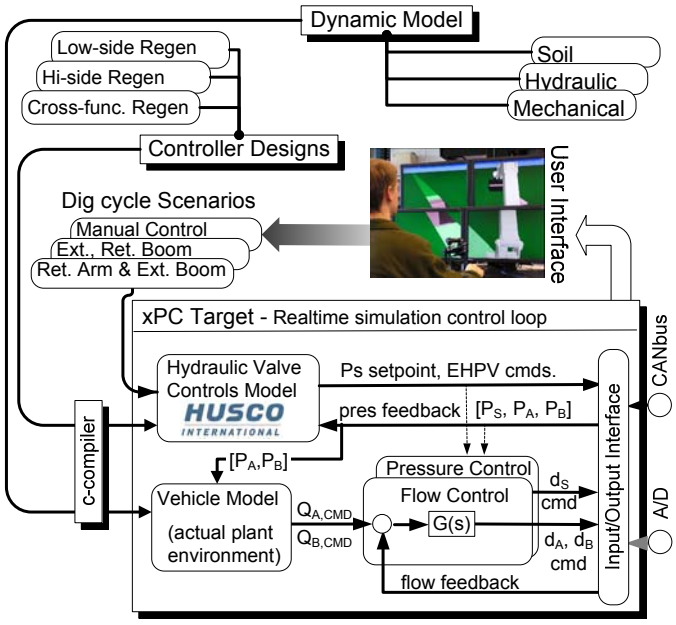

FIGURE 8. ARCHITECTURE OF THE HIL SYSTEM CONTROLLER

Three primary subsystems comprise this software system: executing the Hydraulic Valve Controls Model, simulation of actual plant environment (the Vehicle Model), and low-level HIL testbed controls. The Hydraulic Valve Controls Model reads the measured system pressures (P_S, P_A, P_B, P_R) and the commanded

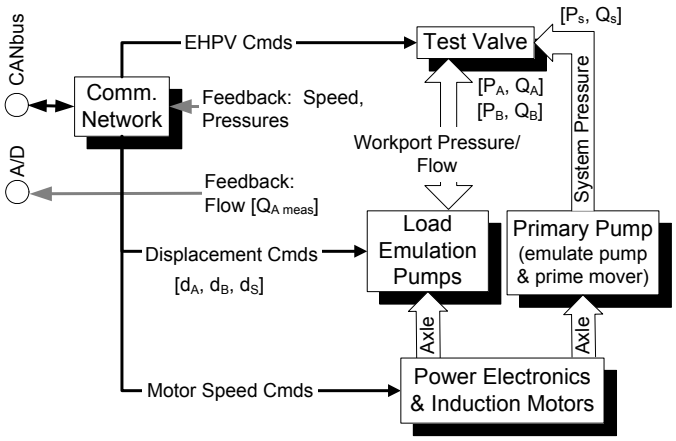

FIGURE 9. CONNECTIONS TO THE HIL HARDWARE

speed of the emulated cylinder (from either a pre-programmed trajectory such as "Retract arm and extend boom" or a real-time operator input), then outputs the EHPV opening commands and $P_{S,\,SETPOINT}$, according to the valve and hydraulic system control logic. Note that the immediate purpose of this HIL testbed is to evaluate different valve controller designs, hence the testbed control system is designed to be capable of on-the-fly changes to the valve controller logic.

Figure 9 shows the connections to the HIL testbed. Note the source of each input: pump displacement commands d_A and d_B result from the low-level Flow Control, which in turn is to track the flow response (Q_A, Q_B) of the Vehicle Model; displacement command d_S is used to cause the system pressure (P_s) to track the reference commanded by the Valve Controls Model.

THE MACHINE MODEL

This section discusses the development and validation of the Vehicle Model (actual plant environment) block depicted in the diagram of Figure 8.

Model Development

Dymola was used to create a multi-domain model of both a hydraulic excavator and a backhoe for use during the HIL simulations, adapted from Beater and Otter [8]. For more information on modeling with open-source hydraulic models created in Dymola, see e.g. Paredis [9]. Figure 10 shows the high-level view of the model, including the rigid-body dynamics of the machine, a pressure-compensated load-sense hydraulic control system, and a dig cycle trajectory block. Close-ups of the PCLS hydraulic model and the rigid body model are provided in Figure 11 and Figure 12, respectively. The hydraulic model accounts for such things as the pump and prime-mover dynamics, 2nd-order valve dynamics (based on information provided by the manufacturer), fluid compliance, and cylinder friction (see Figure 13); higher-order effects including line losses are not modeled. The rigid body model accounts for friction at the joints as well as external loading of the bucket.

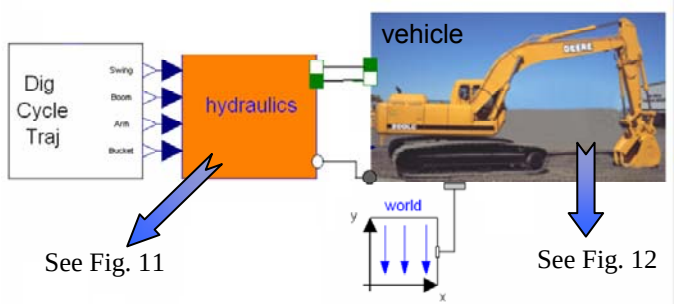

FIGURE 10. DYMOLA BLOCK DIAGRAM OF EXCAVATOR DYNAMICS MODELED IN DYMOLA

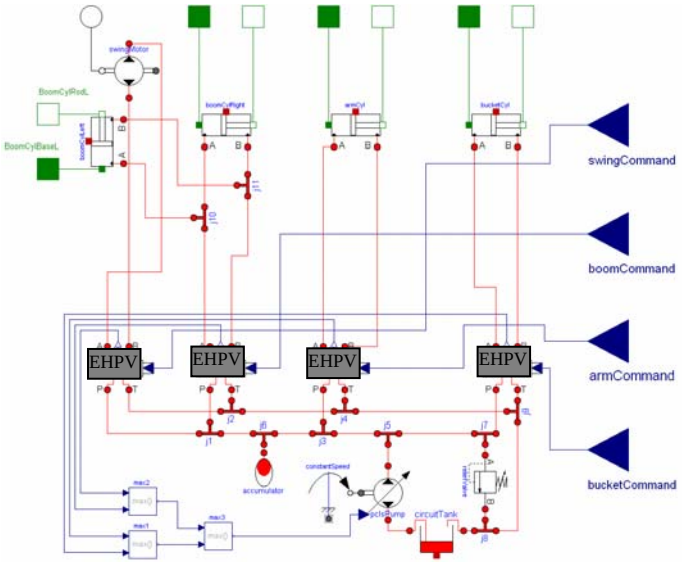

FIGURE 11. MODEL OF PCLS HYDRAULIC SYSTEM WITH INDEPENDENT METERING CONTROL VALVES

Model Validation

Manufacturer's CAD data were used to define the inertial parameters of the rigid body model. The LuGre seal friction model (Figure 13) was used to model the cylinder friction, with the model parameters fit to experimental data recorded on the arm cylinder of an actual machine performing a series of simple "move machine arm in and out" experiments done in free-air.

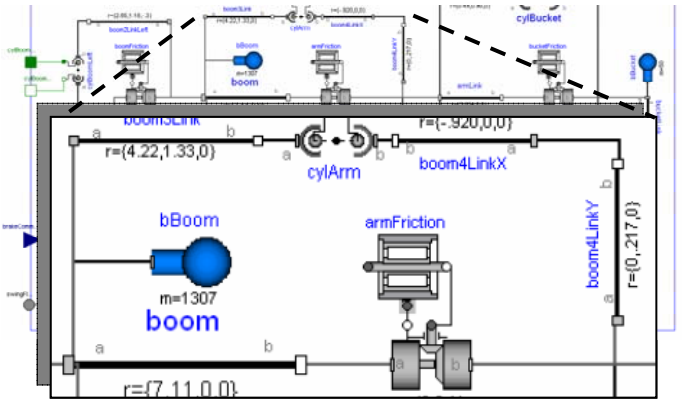

FIGURE 12. EXERPT FROM DYMOLA MODEL OF EXCAVATOR RIGID BODY DYNAMICS

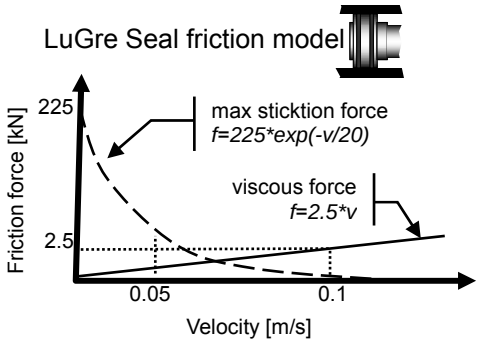

FIGURE 13. CYLINDER FRICTION MODEL WITH PARAMETERS FIT BASED ON EXPERIMENTAL DATA

After this fitting stage, several different sets of experimental data were used to check the simulated response. One representative set of actual and simulated responses, shown in Figure 14, indicates that the model fits the experimental data reasonably well.

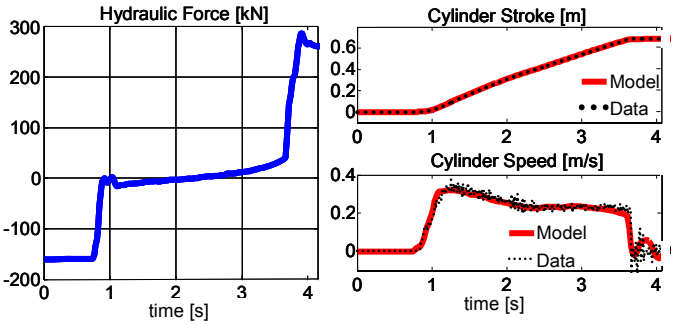

FIGURE 14. LEFT: MEASURED HYDRAULIC FORCE APPLIED TO MODEL. RIGHT: SIMULATED AND ACTUAL MEASURED RESPONSE OF CYLINDER STROKE AND SPEED

The simulated and actual machine pressure responses and valve control commands are shown in Figure 15.

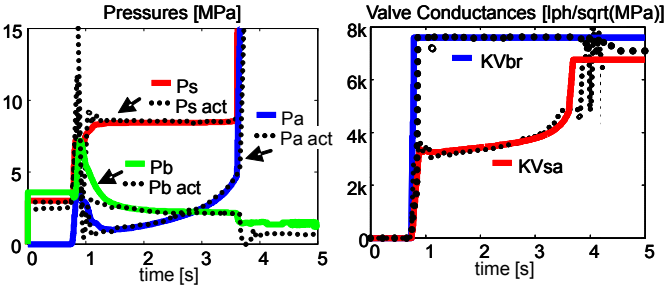

FIGURE 15. LEFT: SIMULATED AND ACTUAL SYSTEM PRESSURES. RIGHT: SIMULATED AND ACTUAL VALVE COMMANDS

HIL SYSTEM PERFORMANCE

The pump model was derived from sets of experimental data recorded with the pump operating in two modes (normal pumping and 'motoring' under an overrunning load) at various pressures and displacements. The experimental data was generated by commanding a sine wave displacement with amplitude approximately 5-percent of the pump's full-scale range. A typical Bode plot of experimental and best-fit model response relating commanded to measured displacement is shown in Figure 16. The best-fit 2nd-order model is

$$G_P = e^{-T_d s}\bar{G}_P, \text{ where } \bar{G}_P = \frac{1}{\left(\frac{s}{24.85}\right)^2 + 1.63\left(\frac{s}{24.85}\right) + 1} \quad (1)$$

with the delay T_d generally in the range of 0.06 to 0.08 seconds.

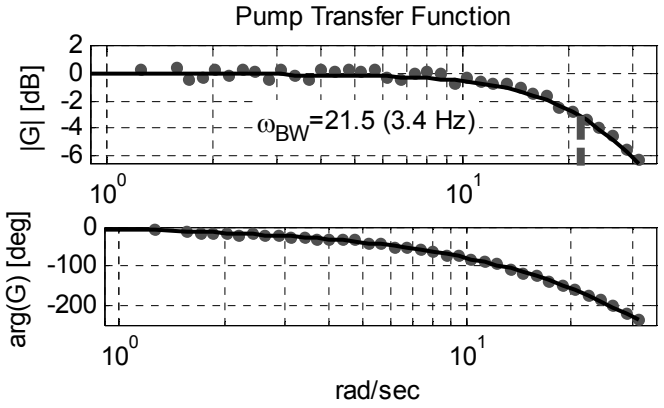

FIGURE 16. EXPERIMENTALLY DERIVED PUMP TRANSFER FUNCTION, G_P

Normalized displacement responses to step commands of varying magnitudes (from 10- to 80-percent of max displacement) and across the range of the pump (operating in normal pumping and motoring modes) are shown by broken lines superimposed in Figure 17. The apparent width of these lines denote the measured uncertainty due to the unknown variable time delay. The solid line is the simulated pump step response based on the model in Eq. 1. This indicates that the pump response is well approximated as linear over the operating range and operating conditions.

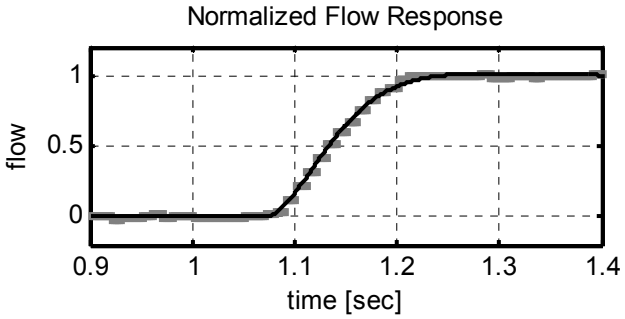

FIGURE 17. (SOLID): STEP RESPONSE BASED ON MODEL DERIVED FROM STEADY-STATE FREQUENCY RESPOSNE. (DASHED): DEPICTS UNCERTAINTY DUE TO VARIABLE TIME DELAY

Closed-loop Pressure (P_S) Control

The Hydraulic Valves Control Model shown in Figure 8 specifies a reference system pressure (P_s) calculated from the simulated valve control logic. A PID-type controller with a feed-forward term controls the HIL system pressure, P_s. The controller is described in the block diagram in Figure 18. The sensed value of P_s is received over CANbus at 100 Hz and pre-filtered at 40 Hz with a first-order filter (C). The pump transfer function, $\bar{G}_P$, is inverted and combined with two fast poles to give a feed-forward term (G_{FF}) which 'overdrives' the pump to improve performance. G_{Lead} and G_{FF} are shown in (2).

$$G_{FF}(s) = \frac{\left(\bar{G}_P\right)^{-1}}{(s/40+1)(s/40+1)},\ G_{Lead}(s) = \frac{K_d s + K_p}{60s+1} \quad (2)$$

The gains K_i, K_d and K_p are calculated using the Zeigler-Nichols tuning method:

$$K_p = 0.6K_c$$
$$K_i = 1.2K_p / T_c$$
$$K_d = K_p T_c / 8$$

where T_c=0.385 [s] and the value of the critical gain K_c is varied in real-time as a function of the actual pump displacement by the switching rule

$$K_c = \begin{cases} K_{c,1} & \bar{D}(s) \geq d_{TH} \\ K_{c,2} & \bar{D}(s) < d_{TH} \end{cases}, \text{ where } \bar{D}(s) = \frac{1}{Ts+1} d_{meas}.$$

The critical switching gains ($K_{c,1}$=2.0 and $K_{c,2}$=3.5), the time constant (T=1 *s*), and the critical displacement threshold (d_{TH}=6 cc/rev) are all chosen empirically to provide stable response across the operating range of the pumps, as was the anti-windup gain (W=7 cc/MPa/s).

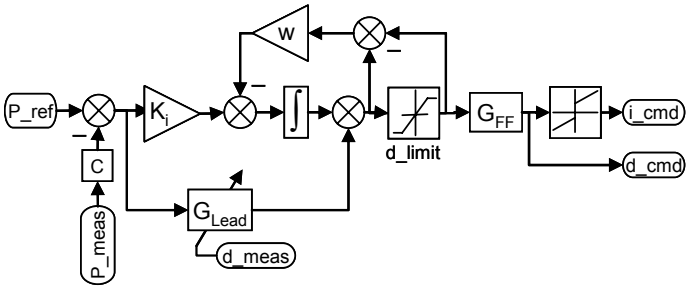

FIGURE 18. PRESSURE CONTROLLER BLOCK DIAGRAM

Frequency response data for the closed-loop control of P_S is shown in Figure 19.

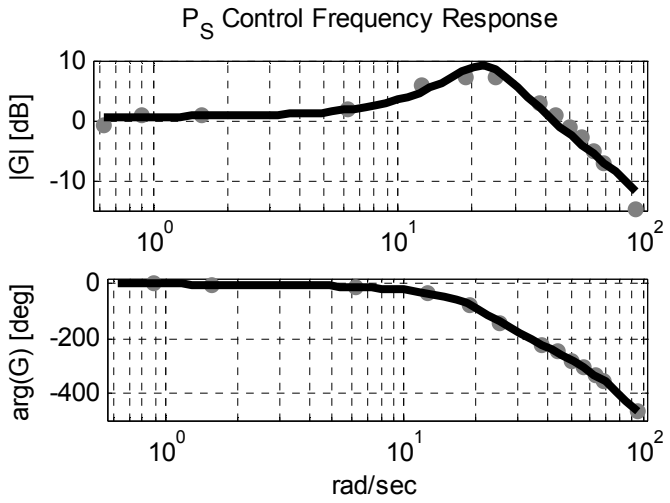

FIGURE 19. FREQUENCY RESPONSE DATA FOR THE CLOSED-LOOP CONTROL OF P_S

The best fit linear system is

$$G_{PS} = \frac{-1.09e^{0.08s}\left(95.51\left(\frac{s}{5.4}\right)^2 + 263\left(\frac{s}{5.4}\right) + 1\right)}{\left(\frac{s}{5.4}\right)^4 - 10.7\left(\frac{s}{5.4}\right)^3 - 20.5\left(\frac{s}{5.4}\right)^2 - 244\left(\frac{s}{5.4}\right) + 1}$$

Experimental step response and disturbance rejection performance for the system pressure regulator are shown in Figure 20. Here, the controller tracks a reference command of P_s=15 MPa by varying the displacement (d_S in Figure 5) to modulate the flow Q_S. The flow passes through EHPVs V1 and V3 (in Figure 5) before draining to tank. A disturbance at 6 s (10 s) occurs when one of the EHPVs is closed (opened) slightly, resulting in a decreased (increased) flow conductance through the valve.

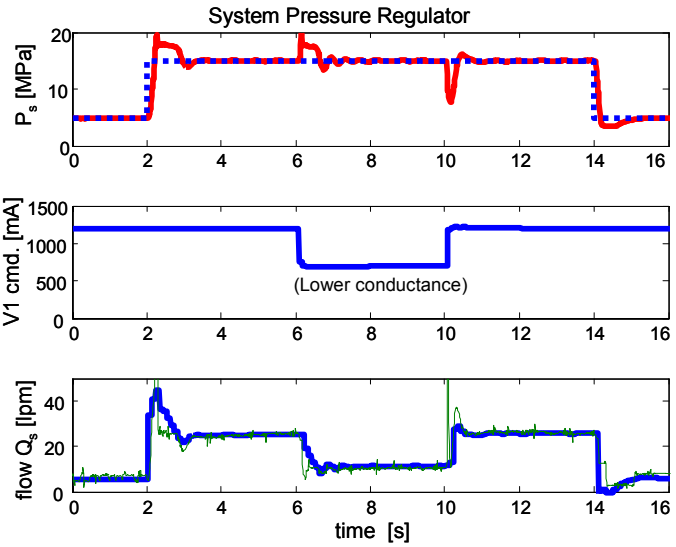

FIGURE 20. STEP RESPONSE AND TYPICAL DISTURBANCE PERFORMANCE OF PRESSURE CONTROLLER

Closed-Loop Flow Control

A closed-loop flow controller controls the workport flow (Q_A, Q_B) in response to the reference calculated by the simulated response of the modeled plant environment. The block diagram for the workport flow controller is shown in Figure 21. This controller consists of a feedforward term compensated for volumetric efficiency of the pump by a look-up table with input dimensions of sensed workport pressure and desired pump displacement. The integral term (K_i=8.5 s^{-1}) accounts for any errors in the feedforward compensation.

The testbed is capable of measuring only the flow Q_A, hence to effectively control flow Q_B, the port B displacement is scaled by the cylinder area ratio ($R=A_a/A_B$) and by an off-line calibration table, L, to account for the pressure-dependent volumetric efficiency of the pump.

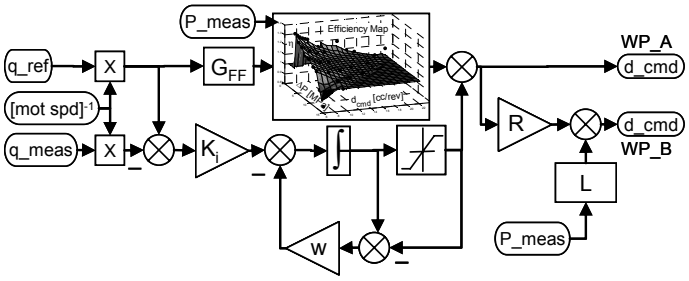

FIGURE 21. FLOW CONTROLLER BLOCK DIAGRAM

The closed-loop frequency response for the control of Q_A and the best-fit linear transfer function for this response are shown in Figure 22 and Equation 3, respectively.

$$G_Q = \frac{e^{-T_d s}}{\left(\frac{s}{68.9}\right)^3 + 3.23\left(\frac{s}{68.9}\right)^2 + 1.92\left(\frac{s}{68.9}\right) + 1} \qquad (3)$$

with the delay T_d generally in the range of 0.06 to 0.08 seconds.

Experimental step response and disturbance rejection performance is shown in Figure 23. Here, P_s is set to a given setpoint and valve V1 is opened; flow Q_A is controlled by actuating the displacement d_A to maintain a set flow reference. At 14 s (18 s) the system pressure is changed from 15 to 10 MPa (10 to 15 MPa); as P_S (and hence P_a) changes, the commanded pump displacement d_A varies to account for pump volumetric inefficiency in order to maintain the flow setpoint.

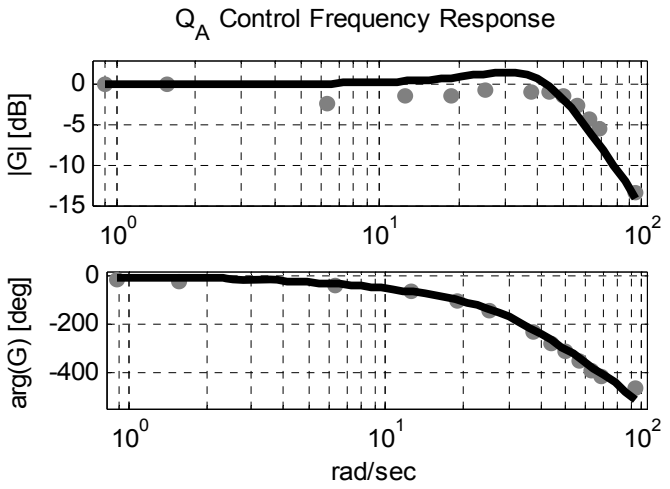

FIGURE 22. FREQUENCY RESPONSE DATA, G_Q, FOR THE CLOSED-LOOP CONTROL OF Q_A

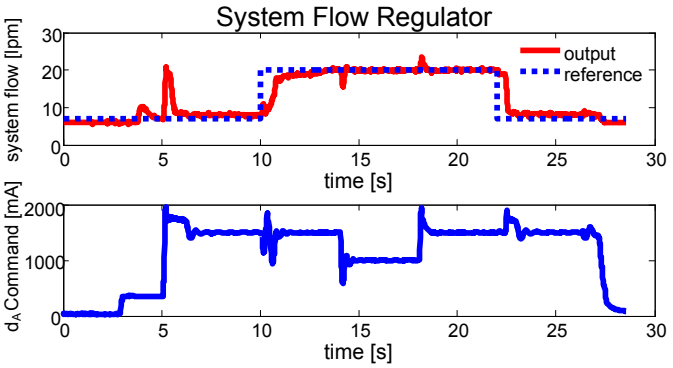

FIGURE 23. STEP RESONSE AND TYPICAL DISTURBANCE PERFORMANCE OF FLOW CONTROLLER

CONLUDING REMARKS

The development of a HIL testbed was discussed, with particular emphasis placed on the testbed control architecture. Initial performance experiments indicate that the testbed is able to be controlled with reasonable accuracy at frequencies below about 3 Hz. With this limit, the testbed is only able to emulate slowly varying dig cycles. Since the gross free-air motion of large construction machines is typically in the range of 1 to 2 Hz, our testbed should be able to emulate these loads well, but is incapable of emulating faster frequencies, such as rigid contact or bucket rap. To this end, future reports will document the ability of the HIL testbed to emulate the loads that correspond to the response of the Vehicle Model to a measured workport pressure of the plant. The fundamental bandwidth limitations are due to stroking speed of the swash plate angle. The load emulation pumps are in the manufacturer's stock configuration and, since this line of pumps typically is used for skid-steer travel applications, the response time is a bit sluggish. Further testbed improvements will address the response speed by modifying the swash plate angle hydraulic control circuitry.

ACKNOWLEDGMENTS

This work was made possible because of the generous support from HUSCO International of Waukesha, Wisconsin. Particular acknowledgment is made to Gus Ramirez, CEO of HUSCO; and to Dwight Stephenson, VP of Engineering at HUSCO. This work was also affiliated with the Center for Compact and Efficient Fluid Power, an Engineering Research Center established through the National Science Foundation.

REFERENCES

[1] J. Pfaff, and K. Tabor, 2004. *Velocity Based Electronic Control System for Operating Hydraulic Equipment*, U. S. Patent 6732512, to HUSCO International, Inc.

[2] K. Tabor, "A Novel Method of Controlling a Hydraulic Actuator with Four Valve Independent Metering Using Load Feedback," in *2005 SAE Commercial Vehicle Engineering Conference*, Rosemont, IL, 2005.

[3] R. Zhang, D. E. Carter, and A. G. Alleyne, "Multivariable Control of an Earthmoving Vehicle Powertrain Experimentally Validated in an Emulated Working Cycle," *American Society of Mechanical Engineers, Dynamic Systems and Control Division (Publication) DSC.* pp. 515-524.

[4] J. L. Lahti, S. J. Andrasko, and J. J. Moskwa, "A Transient Hydrostatic Dynamometer for Single Cylinder Engine Research with Real Time Multi-Cylinder Dynamic Simulation," *American Society of Mechanical Engineers, The Fluid Power and Systems Technology Division (Publication) FPST.* pp. 223-230.

[5] A. J. C. Ramden, J. O. Palmberg, "Design and Analysis of a Load Simulation for Testing Hydraulic Valves," *Fluid Power Engineering: Challenges and Solutions, Tenth Bath International Fluid Power Workshop*, C. R. B. a. K. A. Edge, ed., England: Research Studies Press Ltd., 1998.

[6] S. Driscoll, J. D. Huggins, and W. J. Book, "Electric Motors Coupled to Hydraulic Motors as Actuators for Hydraulic Hardware-in-the-Loop Simulation," *American Society of Mechanical Engineers, The Fluid Power and Systems Technology Division (Publication) FPST.* pp. 111-120.

[7] Dynasim. Dymola, Dynasim Ab, 2008; http://www.dynasim.se. (Available 18 Aug. 2008)

[8] P. Beater, and M. Otter, "Multi-Domain Simulation: Mechancis and Hydraulics of an Excavator," in *3rd International Modelica Conference*, Linkoping, 2003.

[9] C. J. J. Paredis, "An Open-Source Modelica Library of Fluid Power Models," in *Bath/ASME Symposium on Fluid Power & Motion Control (FPMC 2008)*, Bath, UK, 2008.